HIGH-LEVEL SPACECRAFT CHARGING AT GEOSYNCHRONOUS ALTITUDES: A STATISTICAL STUDY

Shu T. Lai
Space Vehicles Directorate
Air Force Research Laboratory
Hanscom AFB, MA 01731-3010

Maurice Tautz
Radex, Inc.

Abstract

We present the results of a statistical study on high-level spacecraft charging at geosynchronous altitudes. Below the critical temperature T* for a surface material, no spacecraft charging occurs. The spacecraft charging potential data are obtained from the ion line of the ion energy spectrum. If the ion line can not be clearly identified, the data point is flagged. We do not use flagged data in our analysis. Since T* depends on the surface material and since each satellite has its own surface material or materials, each satellite is expected to have its own critical temperature. The coordinated space environmental parameter data of the Los Alamos National Laboratory (LANL) geosynchronous satellites include spacecraft charging data measured on several geosynchronous satellites in eclipses and in sunlight over years. We have obtained statistical results of T* for each satellite studied and found that, beyond T*, the high-level spacecraft potential increases almost linearly with the ambient electron temperature. Amazingly, the critical temperature in sunlight remains the same as in eclipse, agreeing with the monopole-dipole differential charging model. This work offers a useful method not only for predicting the onset of spacecraft charging in eclipse and in sunlight but also for predicting high-level spacecraft charging potential with reasonable accuracy at any given ambient electron temperature in the geosynchronous environment.

Introduction

Spacecraft charging can detrimentally affect electrical operations on space systems. Most communication and surveillance spacecraft are at geosynchronous altitudes and many more such spacecraft will be deployed in the new millennium. The plasma density in the geosynchronous environment varies from over 100 cm^{-3} to 0.1 cm^{-3} and the energy varies from a few eV to tens of keV depending on local time and geomagnetic conditions. Spacecraft surface charging occurs at high plasma energies. While surface material properties and spacecraft geometry are defined by spacecraft design, spacecraft charging is controlled by the dynamic plasma condition which varies in time. It is important to identify the most reliable space environment parameters for predicting spacecraft charging.

We have identified the most reliable space environment parameter for predicting spacecraft charging is the plasma electron temperature. Historically, *Rubin et al.* [1980], first reported, though with a few data points only, the linear dependence of spacecraft potential as a function of the ambient electron temperature. Their graph of spacecraft potential versus electron temperature showed an intercept at a finite temperature. *Laframboise et al.* [1982], *Lai et al.* [1982, 1983], and *Prokopenko and Laframboise* [1983] put forth the theory of the critical temperature. Below the critical temperature, spacecraft charging does not occur; above it, spacecraft charging occurs. The theory is now included in standard textbooks on spacecraft-plasma interactions [*Hastings and Garrett*, 1996].

For many years, there was no systematic observation of spacecraft charging together with the coordinated space environment parameters and therefore no way to validate the theory. Recently, the spacecraft charging data obtained on the Los Alamos National Laboratory (LANL) geosynchronous satellites LANL-89-046, LANL-90-95, LANL-91-80, LANL-94-084 and LANL-97A have become available. A recent study [*Lai and Della-Rose*, 2001] using four weeks of spacecraft charging data obtained on LANL-94-084 has uncovered new evidence for the existence of critical temperature of the space plasma electrons for a given spacecraft surface material. Below the critical temperature, little spacecraft charging occurs, while above the critical temperature, the spacecraft potential increases almost linearly. The evidence that a critical temperature exists is abundant and was seen in every charging event on the LANL satellite.

In order to establish the critical temperature theory beyond a doubt, it is necessary to study more data for validation. We report on our results in this paper.

Theory

In the geosynchronous environment, the ambient electron flux exceeds that of the ambient ions by two orders of magnitude, because the electrons are lighter and faster. Measurements on the LANL-94-084 satellite confirmed the flux difference [*Lai and Della-Rose*, 2001].

Suppose a satellite is initially uncharged and the ambient electron temperature is increasing. Eventually, the electron flux increases to a level for charging to occur. At the threshold, the current balance is between the incoming ambient electrons and the outgoing secondary and backscattered electrons.

$$\int_0^\infty dEEf(E) = \int_0^\infty dEEf(E)\left[\delta(E)+\eta(E)\right] \qquad (1)$$

*(E) and 0(E) are the coefficients of secondary electron emission and backscattered electron emission respectively. For a Maxwellian space plasma, the distribution function *f* (E) is of the form:

$$f(E) = n\left(m/2\pi kT\right)^{1/2}\exp\left(-E/kT\right) \qquad (2)$$

Substituting eq(2) into eq(1), one readily obtains two theorems, (I) and (II): -

(I) Since the density *n* is multiplicative, it cancels out on both sides. Therefore, the threshold condition is independent of the plasma density *n*.

(II) The solution T* to eq(1) is the critical temperature for the onset of spacecraft charging.

To solve eq(1), one needs to input the functions *(E) and 0(E). If the ambient electrons are coming in at various angles 2, one needs to use angle dependent functions of *(E,2) and 0(E,2).

Including the angles, the algebra becomes more complicated. The results are given in Table 1.

Table 1. Critical Temperature (keV)

MATERIAL	ISOTROPIC	NORMAL
Mg	0.4	---
Al	0.6	---
Kapton	0.8	0.5
Al Oxide	2.0	1.2
Teflon ©	2.1	1.4
Cu-Be	2.1	1.4
Glass	2.2	1.4
SiO_2	2.6	1.7
Silver	2.7	1.2
Mg Oxide	3.6	2.5
Indium Oxide	3.6	2.0
Gold	4.9	2.9
Cu-Be (Activated)	5.3	3.7
MgF_2	10.9	7.8

Spacecraft Potential

For the onset of spacecraft charging, we have neglected the ions because the ion current is about two orders of magnitude smaller than that of the electrons. However, to determine the resulting spacecraft equilibrium (negative) potential, one needs to include the ions that are attracted. It is often a good approximation to describe the electron repulsion by means of the Boltzmann factor (the exponential term) and the ion attraction by means of the factor of Mott-Smith and Langmuir (the term in parenthesis following the ion current $I_i(0)$) in the following current-balance equation:

$$\Sigma I(\phi) = I_i(\phi) - I_e(\phi) = I_i(0)\left(1 - \frac{q_i\phi}{kT_i}\right) - I_e(0)\exp\left(-\frac{q_e\phi}{kT_e}\right) = 0 \qquad (3)$$

where I_e (N) and I_i (N) are the currents of the repelled and attracted species, respectively, collected by the spacecraft at potential N. Including secondary and backscattered electrons, the electron current I_e(N) in eq(3) is replaced by the net electron current , which is of the form:

$$I_e'(\phi, T_S) = I_e(\phi)\left[1 - <\delta + \eta>\right] \qquad (4)$$

where

$$<\delta + \eta> = \frac{\int_0^\infty dEE\, f(E,T_e)\left[\delta(E) + \eta(E)\right]}{\int_0^\infty dEE\, f(E,T_e)} \qquad (5)$$

Using eq(5), the current-balance equation, eq(3), becomes

$$I_i(0)\left(1 - \frac{e_i\phi}{kT_i}\right) - I_e(0)\,[1 - <\delta + \eta>]\exp\left(-\frac{e_e\phi}{kT_e}\right) = 0 \qquad (6)$$

where the subscripts e and i label electrons and ions, e_e = -e and e_i = e, and e is the elementary charge. For spacecraft potential lower than the ambient ion temperature, that is eN<< kT_i, which is usually valid initially, one expands eq(3.6) in a Taylor series of eN/ kT_i and obtains

$$e\phi = \frac{T_i / T_e}{T_i / T_e + 1} kT_e \log \frac{I_i(0)}{I_e(0)} + \ldots \qquad (7)$$

which gives a straight line of eN as a function of kT. For higher values of eN, the quadratic term needs to be included.

Observations of Spacecraft Charging in Eclipse

The ion to electron temperature ratio T_i/T_e obtained on LANL1994-084 is mostly between 1 and 3 approximately. If the ratio is almost a constant in eq(7), the potential N plotted as a function of kT_e would be almost a straight line. It is not really a straight line, because the log term is also a function of T_e.

The LANL spacecraft potential data are deduced from the shift of the ion distribution f_i(E). Occasionally, the ion shift (ion line) is not clear. Instead of discarding those points which have unclear ion shifts, the LANL team deduced the spacecraft potential for those points in the following manner [*M.F. Thompsen*, personal communication., 2002]. They have observed an empirical curve of spacecraft potential plotted against electron temperature, although they have made no mention of critical temperature. They put the 'unclear' points on this empirical curve according to their electron temperature. Such data are flagged. We have examined the flagged data points in three different months of sample data [courtesy, *M.F. Thompsen*, 2002] and found that the flagged data are all on the sunlight charging curve and none on the eclipse charging curve. Therefore we conclude that the flagged data probably do not affect our eclipse charging study at all.

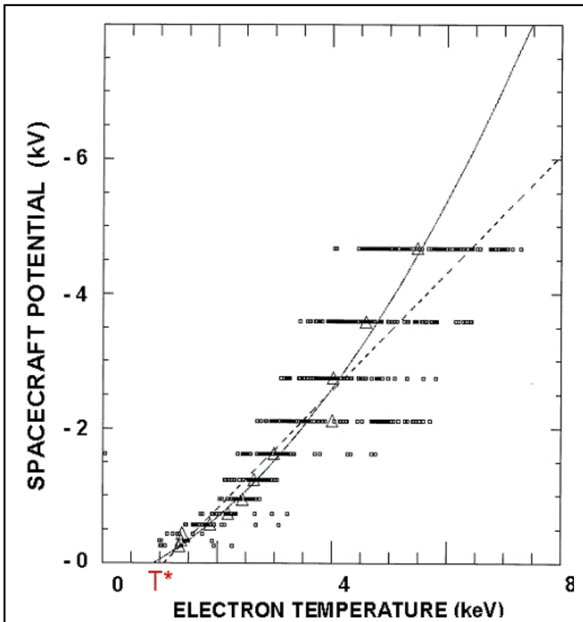

Figure 1 Spacecraft potential and electron temperature measured on LANL-1989-046 during the eclipse periods of Mar 13-28, 1993-2001.

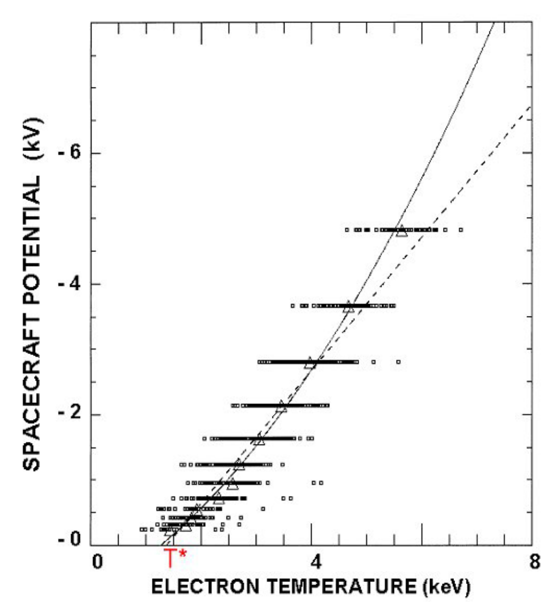

Figure 2 Spacecraft potential and electron temperature measured on LANL-90-095 during the eclipse periods of Mar 14-29, 1993-2001.

Figure 1 shows a plot of LANL 1989-046 spacecraft potential vs. electron temperature for the eclipse periods of Mar 13 to 28, 1993 to2001. Figure 2 shows a similar plot of LANL 1990-095 spacecraft charging and ambient electron temperature data taken in the eclipse periods of Mar 14 to 29, 1993 to 2001. We have also obtained similar results by using eclipse data for the LANL-1994-084, LANL 1991-80 and LANL-1997A satellites. Each of these results shows that (1) the trend of each plot is almost a straight line. (2) there exists an intercept T* (its value being 1.5 to 2 keV approximately), (3) a quadratic function would fit better than a straight line, (4) the values of T* are lower with quadratic fits, but are of the same order of magnitude.

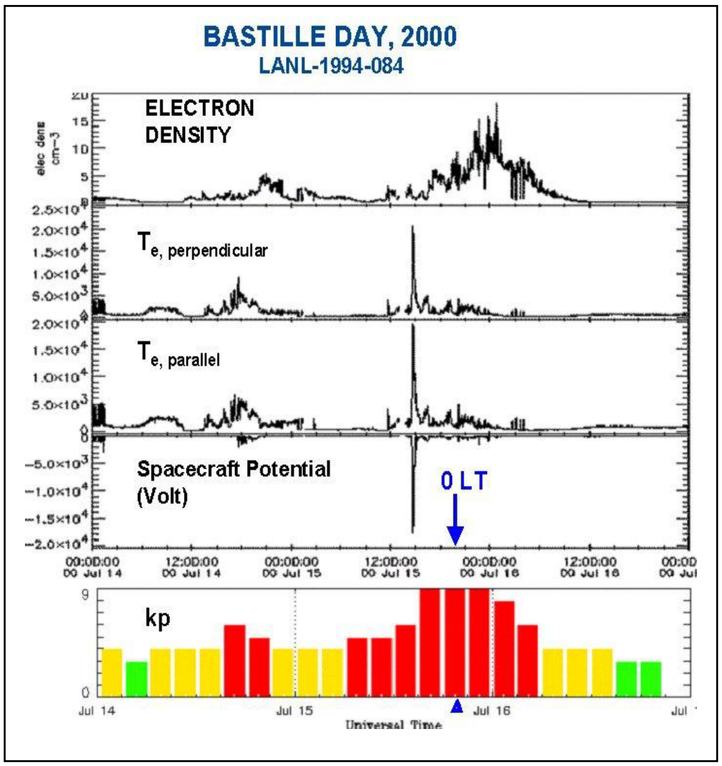

Figure 3. The spacecraft potential mirrors with the electron temperature - not with the electron density or kp.

The most well known storm in the recent solar max was the Bastille Day storm of 2000. Figure 3 shows the magnetic index kp going up to the maximum possible level (k=9) during the storm. The parallel and perpendicular electron temperatures jumped to high values at the arrival of the solar disturbance. The electron density rose later but not simultaneously with the electron temperature. This offers a good opportunity to observe the spacecraft potential in response to these two space parameters, namely, electron temperature and electron density. Indeed, the data measured on LANL 1994-084 shows that the spacecraft potential mirrored the electron temperature but not with the electron density at all. It had been previously assumed that electron flux and electron density were the principal factors.

Spacecraft Charging in Sunlight

Photoelectron emission from spacecraft surfaces often dominates over all other ambient currents. Therefore, it seems impossible for spacecraft to charge to negative potentials in sunlight. Yet, the LANL satellites often charge to hundreds or thousands of negative volts in sunlight. We are going to present that the LANL satellite charging data agree well with the monopole-dipole model.

In the following, we will present an important finding: "The level of spacecraft charging in sunlight is usually about 1/3 of that in eclipse". As a collorary, we have another important finding: "The onset of spacecraft charging occurs at the same critical temperature no matter the satellite is in clipse or in sunlight."

Photoelectron Current in Sunlight

Laboratory measurements show that typical spacecraft surface materials generate in space conditions photoemission currents of the order of $J_{ph} = 2x10^{-9}$ A/cm^2 [*Stannard, et al.*, 1978]. For comparison, the average electron current density measured on the SCATHA (Spacecraft Charging at High Altitudes) satellite was $<J> = 0.115x10^{-9}$ A/cm2 [*Purvis and Garrett*, 1984]. Thus, the photoemission current density J_{ph} exceeds the average ambient electron current J by a factor F = 20.

$$I_{ph} = 20 < J > \qquad (8)$$

If a spacecraft is charged to a negative potential in steady state, the potential must satisfy the current balance equation. For example, current balance in the Mott-Smith and Langmuir model is of the form:

$$I_e(0)\exp\left(-q_e\phi / kT_e\right) - I_i(0)\left(1 - \frac{q_i\phi}{kT_i}\right) = I_{ph} \qquad (9)$$

where the notations are as usual, q_e = -e, q_i = e, and is negative. If $I_{ph} > I_e(0)$, there is no solution for the above equation. How, then, can spacecraft charging to negative potentials occur?

Monopole-Dipole Potential in Sunlight

Consider a negatively charged satellite with dielectric surfaces in sunlight. The shadowed side charges to a higher (negative) potential than the sunlit side. Taking the first two terms of an infinite series in Legendre function of a general potential distribution, one obtains a monopole-dipole potential distribution [*Besse and Rubin*, 1980]:

$$\phi(\theta, R) = K\left(\frac{1}{R} - \frac{A\cos\theta}{R^2}\right) \qquad (10)$$

where A is the dipole strength which is less than unity. The angle 2 = 0^o is the normal sunlight direction (Figure 4). We have conducted an explicit validation, for the first time, of the monopole-dipole distribution in sunlight charging.

For unit radii satellite, the radial distance R=1 at the satellite surface, and K = N(90^o, 1) equals the monopole potential. The potential barrier is located at R_S, where the potential is the maximum for 2 = 0^o .

$$\left[\frac{d\phi(0^o,R)}{dR}\right]_{R=R_S}=0 \qquad (11)$$

which gives $R_S = 2A$. Therefore, $A > ½$, otherwise the barrier is located inside the spacecraft.

The barrier height B is given by

$$B=\phi(0^o,R_S)-\phi(0^o,1)=K\frac{(2A-1)^2}{4A} \qquad (12)$$

The fraction f of photoelectron flux (Figure 5) escaping through the potential barrier is given by

$$f=\frac{\int_B^\infty dEE\exp(-E/kT)}{\int_o^\infty dEE\exp(-E/kT)}=\left(\frac{B}{kT}+1\right)\exp\left(-\frac{E}{kT}\right) \qquad (13)$$

where the photoelectron distribution is Maxwellian and has a typical temperature T of 1.2 eV [*Whipple*, 1982]. Since the photoelectron temperature is low, very small barrier height will block most of the photoelectrons.

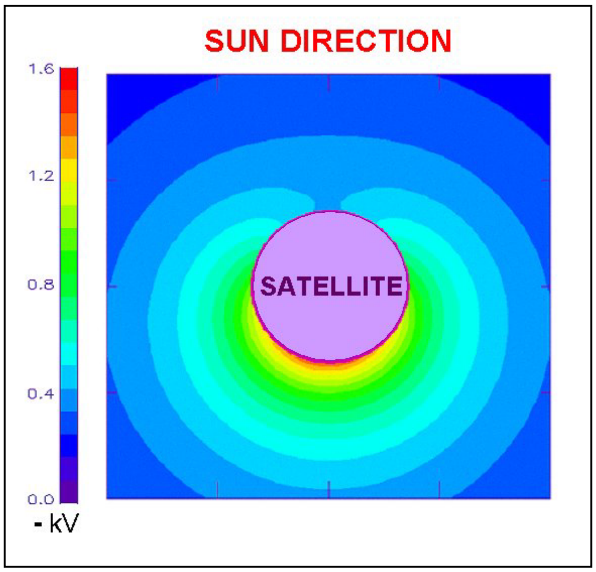

Figure 4. Typical potential contours in a monopole-dipole potential distribution. The contours wrap from the dark side to the sunlit side.

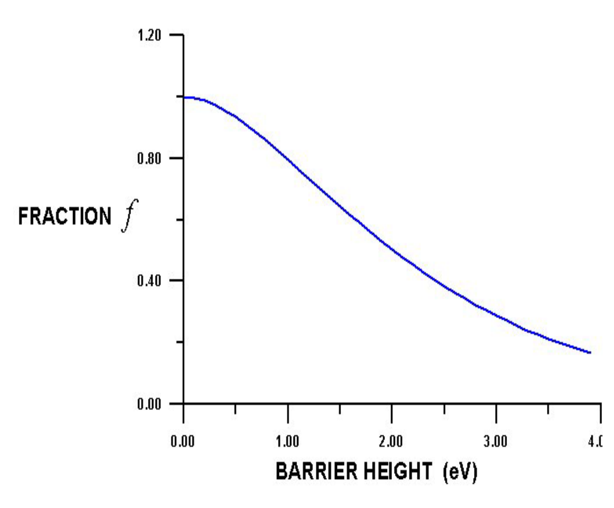

Figure 5. Fraction of photoelectron current escaping through the barrier. A small barrier height is sufficient to block most of the photoelectron current.

In particular, for high level charging, the ratio B/K of the barrier potential to the monopole potential is usually nearly zero. Substituting B/K ≈ 0 in eq(12) gives A ≈ ½. As a result, the ratio of the sunlit surface potential to that of the shaded surface is given by (Figure 6):

$$\frac{\phi(0^o,1)}{\phi(180^o,1)} = \frac{1-A}{1+A} = \frac{1-1/2}{1+1/2} = \frac{1}{3} \qquad (14)$$

Observations of Spacecraft Charging in Sunlight

We have analyzed several years of the Los Alamos National Laboratory (LANL) satellite charging data and obtained very useful statistical results on the behavior of charging in sunlight. The results agree surprisingly well with the monopole-dipole model.

Figure 7 presents a compilation of charging data obtained on the LANL 1991-80 Satellite for the period March 13-28, 1994-2001. The March period is chosen because of the following reason. The geosynchronous satellite, being in the equatorial plane, undergoes eclipse around midnight in March and September. Therefore, both eclipse charging and sunlight charging data are available for comparison during the March period. A statistical curve fit shows clearly that there are two trends in Figure 7. The ratio of the potentials in eclipse and in sunlight is approximately 1/3. For example, when the sunlight charging potential is -1 kV at electron temperature of about 4.4 kV, the eclipse charging potential at the same temperature is about -3 kV . This result is a strong evidence supporting the validity of the monopole-dipole model.

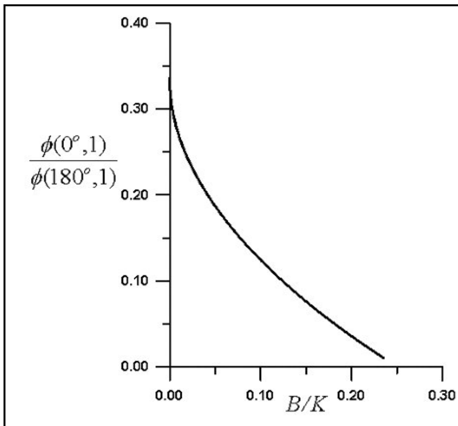

Figure 6. Ratio of potentials of sunlit and shadowed surfaces as a function of barrier potential.

Since 1/3 of a finite number is finite while 1/3 of zero is obviously zero, the onset of spacecraft charging occurs at the same critical temperature of the space plasma electrons. Below the critical temperature, there is no charging. Above it, the charging level increases with the temperature. This new and important finding is clearly seen in Figure 7.

To add more credence to the above findings, we present another statistical graph (Figure 8) showing the charging data of a different satellite, viz., LANL-1997A, during the periods September 14-28, 1997-2001. Again, the period September 14-28 is chosen because both eclipse charging and sunlight charging events are available for comparison. In Figure 8, the ratio of potentials in sunlight to that in eclipse is again approximately 1/3. For example, the sunlight charging potential is about -1 kV at the temperature of about 4.4 kV; that of the elipse charging at the same temperature is about -3 kV. The onsets of eclipse charging and sunlight charging occur at approximately the same value of critical temperature. Similar results have been obtained for the other LANL satellites. We conclude that these results strongly support the validity of the monopole-dipole model.

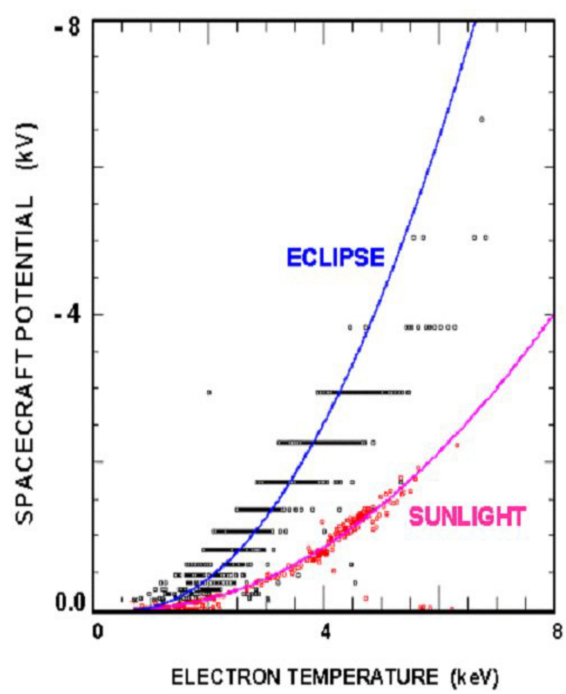

Figure 7. Charging voltage in sunlight is 1/3 that in darkness.

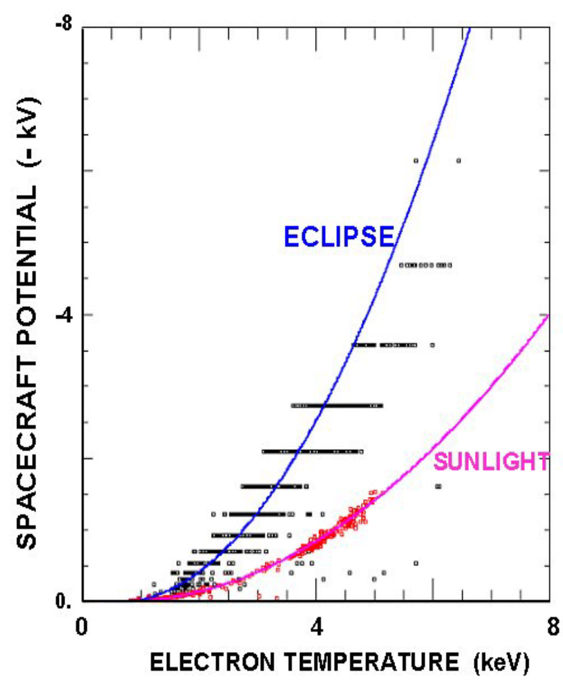

Figure 8. Charging voltage in sunlight is 1/3 that in darkness.

Summary and Discussion

The geosynchronous altitudes are the most important region for spacecraft charging. Most communication satellite are there, while the ambient plasma varies in temperature and density depending on the local time and space weather. A most important problem is to seek the most reliable space environment indicator of the onset of spacecraft charging. By studying the LANL geosynchronous satellite data, we have found that spacecraft charging depends strongly on the ambient plasma electron temperature, and not as much on the other space environment parameters such as electron density, ion temperature, ion density, and even high kp. The exact level of charging depends on the spacecraft geometry, configuration of surfaces, etc. The average potential is, however, almost a straight line as a function of temperature. The line deviates from being absolutely straight, because there is a quadratic term in the Taylor series of potential as a function of temperature and, furthermore, the plasma distribution may resemble a kappa distribution at high temperatures.

It has long been known from laboratory measurements that the photoemission flux from sunlit surfaces should exceed the ambient plasma electron flux at geosynchronous altitudes. How then can satellites charge to negative voltages? To solve this problem, one realizes that there is always a shadowed surface when a satellite is in sunlight. High negative charging can occur on the shadowed surface when the plasma electron temperature is hot.

A bootstrap mechanism then occurs as follows. The negative potential contours extend from the high voltage (dark) side to the low voltage (sunlit) side, thereby trapping the photoelectrons with a potential barrier. Since photoelectrons have a few eV only in energy, a small potential barrier is sufficient to trap most of the photoelectrons. With photoemission partly suppressed, the sunlit side can charge to high negative potentials. The results of the monopole-dipole model predicts that the ratio between the eclipse charging potential to the sunlit charging potential under the same space plasma conditions is approximately 1/3.

Amazingly, we have found abundant evidence that this ratio is valid statistically by studying years of charging data obtained on LANL satellites, . Since R of a finite number is finite and R of a zero is zero, the critical temperature for the onset of spacecraft charging is therefore unchanged - it is the same whether in eclipse or in sunlight. We believe that this is a significant finding for developing a reliable indicator in the future for predicting spacecraft charging in changing space weather.

Acknowledgment

The Los Alamos Magnetospheric Plasma Analyzer (MPA) measurements were obtained from the CDAWeb data service at NASA Goddard Space Flight Center. We thank M. Thomsen for permission to use the MPA data.

References

1. Besse, A.L. and A.G. Rubin, A simple analysis of spacecraft charging involving blocked photo-
2. electron currents, J. Geophys. Res., **85**, 2324-2328, 1980.

3. Hastings, D., and Garrett, H.B., Spacecraft-Environment Interactions, Cambridge University Press, Cambridge, UK., 1997.

4. Laframboise, J.G., Godard R. and Kamitsuma M., Multiple Floating Potentials, Threshold Temperature Effects, and Barrier Effects in High Voltage Charging of Exposed Surfaces on Spacecraft, in Proceedings of International Symposium on Spacecraft Materials in Space Environment, Toulouse, France, 1982, pp.269-275.

5. Laframboise, J.G. and Kamitsuma, M., The Threshold Temperature Effect in High Voltage Spacecraft Charging, in Proceedings of Air Force Geophysics Workshop on Natural Charging of Large Space structures in Near Earth Polar Orbit, AFRL-TR-83-0046, ADA-134-894,1983, pp .293-308.

6. Lai, S.T., H.A. Cohen, T.L. Aggson and W.J. McNeil, Charging of booms on a satellite rotating in sunlight, J. Geophys. Res., **91**, No.A11, 12137-12141, 1986.

7. Lai, S.T., Gussenhoven, M.S. and Cohen, H.A., Energy Range of Ambient Electrons Responsible for Spacecraft Charging, EOS Trans. Am. Geophys. U., Vol.63, No.18, 1982, pp.421.

8. Lai, S.T., Gussenhoven, M.S., and Cohen, H.A., The Concepts of Critical Temperature and Energy Cutoff of Ambient Electrons in High Voltage Charging of Spacecraft, in Proceeedings of the 17th ESLAB Synposium, edited by D.Guyenne and J.H. A. Pedersen, pp. 169-175, European Space Agency, Noordwijk, The Netherlands, 1983.

9. Lai, S.T., Spacecraft Charging Thresholds in Single and Double Maxwellian Space Environments, IEEE Trans. Nucl. Sci., Vol.19, 1991, pp.1629-1634.

10. Lai, S.T. and D. Della-Rose, Spacecraft charging at geosynchronous altitudes: New evidence of existence of critical temperature, J. Spacecraft & Rockets, Vol.38, pp.922-928, Dec., 2001.

11. Purvis, C., H.B. Garrett, A.C. Whittlesey and N.J. Stevens, Design guidelines for assessing and controlling spacecraft charging effects, NASA Tech. Paper 2361, 1984.

12. Prokopenko, S.M. and Laframboise J.G.L., High Voltage Differential Charging of Geostationary Spacecraft, J. Geophys. Res., Vol. 85, No.A8, 1980, pp.4125-4131.

13. Rubin, A., Garrett, H.B., and Wendel, A.H., Spacecraft Charging on ATS-5, Air Force Geophysics Laboratory, AFGL-TR-80-0168, ADA-090-508, 1980.

14. Stannard, P.R., et al., Analysis of the charging of the SCATHA (P78-20) satellite, NASA CR-165348, 1981. Sanders, N.L.and G.T.Inouye, Secondary Emission Effects on Spacecraft Charging: Energy Distribution Consideration, in Spacecraft Charging Technology 1978, edited by R.C.Finke and C.P. Pike, pp. 747-755, AFGL, Hanscom AFB., Massachusetts, 1978. NASA-2071, ADA ADA-084626.

15. Whipple, E.C., Potentials of surfaces in space, Reports on Progress in Physics, vol. 44, pp.1197-1250, 1981.